Energy gauge and electron confinement in quasicrystals

1998 J. Phys. A: Math. Gen. 31 743

(http://iopscience.iop.org/0305-4470/31/2/029)

J. Phys. A: Math. Gen. **31** (1998) 743–756. Printed in the UK PII: S0305-4470(98)81379-6

Energy gauge and electron confinement in quasicrystals

Peter Kramer

Institut für Theoretische Physik der Universität, Tübingen, Germany

Received 28 January 1997, in final form 1 September 1997

Abstract. Electronic single-particle states in 1D finite, periodic and quasiperiodic potentials are analysed. The notions of band germs, Bloch germs, bound and decaying states and of energy gauges are introduced and illustrated by exact solutions with the continuous transfer matrix.

1. Global and local views of the electronic structure

In the physics of quasicrystals [7] the electronic structure is a central issue. From its analysis one expects insight into the stability of these phases, for example through the Hume–Rothery mechanism, and an understanding of the extremely low conductivity found at low temperature in these metallic systems.

Much effort has been devoted to the computation of the density of electronic states (DOS) in quasicrystals. Theoretical studies of the DOS made in particular by Fujiwara *et al* [3, 4] employ band structure computations of LMTO type [13]. When applying band-structure computations to quasicrystals one must replace the quasiperiodic structure globally by a periodic approximant with a single but large unit cell with a *large-scale arrangement* of many atoms. The resulting DOS then reflects a complex many-band structure. The computations show two features: a pseudogap near the Fermi energy, and a spiky structure of the DOS. Both features were proposed as characteristics of quasicrystals, but are still controversial: recent experimental photoemission data with ultrahigh resolution obtained by Stadnik *et al* [14] confirm the pseudogap but yield, in contrast to the theoretical prediction, a very smooth behaviour of the DOS. For the theory the question arises concerning which limitations of the computed electron structure are due to the global-band approximation.

In structure models, quasicrystals are often described as a quasiperiodic arrangement of a few local atomic clusters. This brings up the question of *local views on the electronic structure in quasicrystals*. Heine [5] has advocated a radical *local viewpoint* on general electronic structures in solids and proposed to throw out K-space. The recursive method [6] is a computational approach along this line. We shall adopt a local view but emphasize that this does not exclude K-space. A local viewpoint was expressed earlier in the cellular method for crystals due to Wigner and Seitz [15]: the one-electron Schrödinger equation is to be solved locally on the Wigner–Seitz cell of the crystal with Bloch-type boundary conditions. These boundary conditions display a *local role* of the K-space. In a crystal the local Bloch states on the cells match together to form the global-band states. The computational problem with the cellular method is that the Bloch boundary conditions in three dimensions (3D) cannot be handled exactly so that approximations are required, see [1].

0305-4470/98/020743+14$19.50

An analysis free from approximations is available in one dimension (1D). Here one can use the transfer matrix and the trace map [2]. All the quantum multiple and backscattering effects of the electrons from the atomic potentials are treated exactly. In 1D the cellular method works exactly, for example for the well known Kronig–Penney model. The appearance of quasicystals has suggested many studies of 1D quasiperiodic sequences from several cells, see Kohmoto [8] for the discrete case and work quoted in [2] for the continuous one. As in the cellular method, one starts from local states on several cells with K-type boundary conditions for each cell. Then one must match these boundary conditions over a quasiperiodic string with several cells of increasing length.

In this paper we reexamine the electronic states in periodic and in quasiperiodic 1D potentials. We start from a local point of view and stress boundary conditions. Our treatment differs from former work in 1D by the emphasis on an *exact tight-binding scenario* defined in sections 3 and 4. In sections 4 and 5 we propose the local concepts of *band germs, Bloch germs, energy gauges and decaying states* and analyse them in sections 6 and 7 on very simple models with one type of (atomic) δ-potentials with two spacings. We believe that these concepts are relevant for the interpretation of electrons in three dimensional (3D) quasicrystals, although we cannot yet propose a computational scheme for them.

2. Transfer matrices

For the mathematical physics of 1D quantum systems we refer to [12]. Consider electron states on the line as solutions of the time-independent continuous Schrödinger equation with V a piecewise constant potential and with energy E. Arrange solutions and their derivatives into columns. A fundamental system of two solutions and their derivatives can be put into the two columns of a 2×2 *transfer matrix* $M(x)$. As initial data for the system we take

$$M(0) = \begin{bmatrix} 1 & 0 \\ 0 & 1 \end{bmatrix}. \tag{1}$$

Then the Wronski determinant of the transfer matrix $M(x)$ keeps the initial value $W = 1$. A general transfer matrix is a product of factors which apply to intervals with constant potential. Matrix multiplication guarantees continuity of the solutions and their first derivatives. Typical factors of a general transfer matrices are the *square well of length* a,

$$M(a) = \begin{bmatrix} \cos(ka) & k^{-1}\sin(ka) \\ -k\sin(ka) & \cos(ka) \end{bmatrix}. \tag{2}$$

Here the potential is $V_0 = -\frac{\hbar^2}{2m}\rho^2$ and the energy is $E = -\frac{\hbar^2}{2m}\kappa^2 < 0, k^2 + \kappa^2 = \rho^2$.

In the limit $k^2 a = u, ka \to 0$ the square well goes into the *attractive* δ*-well* of strength u which we indicate by an argument ϵ,

$$M(\epsilon) = \begin{bmatrix} 1 & 0 \\ -u & 1 \end{bmatrix}. \tag{3}$$

The transfer matrix

$$M(b) = \begin{bmatrix} \cosh(\kappa b) & \kappa^{-1}\sinh(\kappa b) \\ \kappa\sinh(\kappa b) & \cosh(\kappa b) \end{bmatrix} \tag{4}$$

forms a *barrier* of length b if the potential is $V_0 = \frac{\hbar^2}{2m}\rho^2$ and the energy is $E = \frac{\hbar^2}{2m}k^2 > 0, k^2 + \kappa^2 = \rho^2$. The corresponding δ*-barrier* is obtained by replacing $u \to -u$ in equation (3). We keep the transfer matrix of equation (4), but now take $V_0 = 0$ and $E = -\frac{\hbar^2}{2m}\kappa^2$. Then $M(b)$ describes a *tunnel of length* b.

The transfer matrices are elements of the real unimodular group $SL(2, R)$, [12, 9]. The equivalence classes of this group *fall into three types* characterized by the absolute values of their traces: $\frac{1}{2}|\operatorname{tr}(M)| < 1, > 1, = 1$. The first case yields for the eigenvalues two complex conjugate numbers of modulus 1, the second two real numbers with product 1, and the third case allows for a Jordan decomposition.

The occurrence of complex eigenvalues motivates the use of *the complex form* $SU(1, 1)$ of the group $SL(2, R)$ [9, 10], defined by $q^{\dagger}SL(2, R)q$ with elements g_c,

$$\begin{aligned} g_c &:= q^{\dagger} g q \\ q &:= \sqrt{\frac{1}{2}} \begin{bmatrix} 1 & 1 \\ \mathrm{i} & -\mathrm{i} \end{bmatrix}. \end{aligned} \tag{5}$$

For a case $g_c : \frac{1}{2}\operatorname{tr}(g_c) = \lambda_0, |\lambda_0| < 1$ with complex conjugate eigenvalues

$$\mu = \lambda_0 + \mathrm{i}\sqrt{1 - {\lambda_0}^2} \qquad \overline{\mu} = \lambda_0 - \mathrm{i}\sqrt{1 - {\lambda_0}^2} \tag{6}$$

the diagonalizing matrix can be chosen from $SU(1, 1)$ in the form

$$V_c = \begin{bmatrix} v & \overline{w} \\ w & \overline{v} \end{bmatrix} \qquad v\overline{v} - w\overline{w} = 1. \tag{7}$$

The eigenvalue equation for complex g_c,

$$g_c V_c = V_c \Delta \qquad \Delta := \begin{bmatrix} \mu & 0 \\ 0 & \overline{\mu} \end{bmatrix} \tag{8}$$

yields for the real form g from equation (5) the eigenvectors in the form

$$g(qV_c) = (qV_c)\Delta. \tag{9}$$

Apply this to the transfer matrix $g = M$. Then the columns of $M' = M(qV_c)$ can be interpreted as *a new system of fundamental solutions with initial data given by* (qV_c). If we compute the charge current density of the two column states ϕ_1, ϕ_2 of $M(qV_c) = (qV_c)\Delta$, we obtain from equation (7), (see appendix A1),

$$j_1 = -j_2 = \frac{e\overline{h}}{2\mathrm{i}m}(\overline{\phi_1}\phi_1{}' - \overline{\phi_1}{}'\phi_1) = \frac{e\overline{h}}{2m}. \tag{10}$$

Proposition 1. For a real transfer matrix with $\frac{1}{2}|\operatorname{tr}(M)| < 1$, we can determine two complex eigenvectors with standard charge densities of opposite signs.

From equation (7) it can easily be shown that *for any linear combination of the type* $\phi = \phi_1 + \exp(\mathrm{i}\alpha)\phi_2$ *the charge current density is* $j = 0$.

3. Loose and tight binding

Consider in 1D a finite number of δ-barriers arranged at relative distances $a, b, c \ldots$. With $E > 0$, the potentials between two consecutive barriers may model attractive potentials of atoms. The atomic potentials have the width of the intervals. At the limits of these intervals, they are separated only by the weak δ-barriers . We call this a *loose binding*. This scenario has been very popular for the consideration of electrons in quasiperiodic 1D potentials.

It is well known that the tight-binding approximation in 3D, based on bound atomic orbitals, gives a very successful account of electrons in crystals. Consider in 1D a finite number of attractive δ-potentials arranged at relative distances $a, b, c, \ldots$. Take electron states in these attractive atomic potentials at negative energy $E < 0$. In contrast to the loose binding scenario there will be bound states. An electron must cross a tunnel to reach the

next atom. We refer to this situation as the exact *tight-binding scenario*, but strictly avoid any approximation such as atomic orbitals which are often associated with this scheme.

In what follows we shall study the tight-binding scenario in more detail.

4. Tight binding: band germs and tunnels

In contrast to the usual treatment we consider *states on finite strings*. A typical string of the tight-binding scheme is a *potential well* of length a, followed by an interval of length b with potential $V = 0$ which for $E < 0$ represents a *tunnel of length* b. Its transfer matrix from equations (2) and (4) is

$$M(b+a) = \begin{bmatrix} \cosh(\kappa b) & \kappa^{-1}\sinh(\kappa b) \\ \kappa\sinh(\kappa b) & \cosh(\kappa b) \end{bmatrix} \begin{bmatrix} \cos(ka) & k^{-1}\sin(ka) \\ -k\sin(ka) & \cos(ka) \end{bmatrix} \tag{11}$$

where the energy is now $E = -\frac{\hbar^2}{2m}\kappa^2$ and $k^2+\kappa^2 = \rho^2$. Replacing the well by a δ-potential we obtain

$$\begin{aligned} M(b+\epsilon) &= \begin{bmatrix} \cosh(\kappa b) & \kappa^{-1}\sinh(\kappa b) \\ \kappa\sinh(\kappa b) & \cosh(\kappa b) \end{bmatrix} \begin{bmatrix} 1 & 0 \\ -u & 1 \end{bmatrix} \\ &= \begin{bmatrix} \cosh(\kappa b) - \frac{u}{\kappa}\sinh(\kappa b) & \kappa^{-1}\sinh(\kappa b) \\ \kappa\sinh(\kappa b) - u\cosh(\kappa b) & \cosh(\kappa b) \end{bmatrix}. \end{aligned} \tag{12}$$

By the argument $(b+\epsilon)$ we indicate the presence of a δ-well at $x = 0$.

Definition 2. For a product of the type in equations (11) and (12), a range of negative energies $E < 0$ such that $\frac{1}{2}|\operatorname{tr}(M)| \leqslant 1$ we call a *band germ*.

A band germ, derived from a local attractive potential and tunnel, is a negative-energy range which allows for specific boundary conditions. The one-electron states in the attractive potential followed by the tunnel allow us to introduce a band germ label $K(E)$ by putting

$$\tfrac{1}{2}\operatorname{tr}(M) = \tfrac{1}{2}(\mu + \overline{\mu}) := \cos K(a+b), 0 \leqslant K(a+b) < \pi. \tag{13}$$

Example 1. To find the band germs in the example of the well equation (11) we look in particular for the energy where

$$\begin{aligned} &\frac{1}{2}\operatorname{tr}(M(b+a)) = \cosh(\kappa b)\cos(ka) - \frac{1}{2}\left(\frac{k}{\kappa} - \frac{\kappa}{k}\right)\sinh(\kappa b)\sin(ka) = 0 \\ &\coth(\kappa b)\cot(ka) = \frac{1}{2}\left(\frac{k}{\kappa} - \frac{\kappa}{k}\right). \end{aligned} \tag{14}$$

Since the transfer matrix is a continuous function of the energy, we can expect that any energy value $E = -\frac{\hbar^2}{2m}\kappa^2$ obeying equation (14) forms the *centre of a band germ* such that $-1 < \frac{1}{2}\operatorname{tr}(M) < 1$. With $\cot(\alpha) := \frac{k}{\kappa}$ we introduce an angle on the circle given by $k^2 + \kappa^2 = \rho^2$. The condition (14) becomes

$$\coth(\kappa b)\cot(ka) = \cot(2\alpha). \tag{15}$$

This equation has at least one, in general several, solutions and so we can find the band germs. We characterize the states belonging to a band germ in terms of the finite string.

Proposition 3. For any energy within a band germ, there are two complex eigensolutions of M which after passing the string would be multiplied by two eigenvalues $\mu, \overline{\mu}, \mu\overline{\mu} = 1$ respectively. These we call the *Bloch germs*.

5. An energy gauge for bound and decaying states

Definition 4. Consider a finite string and embed it into tunnels of infinite length both to the right and to the left. A *bound state* is a solution of negative energy $E = -\frac{\hbar^2}{2m}\kappa_0^2$ which decays in the tunnels to the right and to the left as $\exp(\mp\kappa_0 x)$ respectively.

We emphasize that bound states can occur only in the tight-binding, not in the loose-binding scenario. To characterize bound states on a finite string we pass to a different representation. The transfer matrix is nonlinearly related to the *scattering matrix* $S(k)$ [9]. Bound states appear in the analytic continuation $k \to \mathrm{i}\kappa$ both of the transfer and the scattering matrix from $E > 0$ to $E < 0$: assume that $V \neq 0$ only in a bounded interval and consider $E < 0$. Then to the left and to the right of this interval take *tunnels* of infinite length with transfer matrices of the type of (4) but with energy $E = -\frac{\hbar^2}{2m}\kappa^2$. Pass in these transfer matrices equation (4) from hyperbolic solutions to increasing and decreasing exponential solutions respectively. This is achieved by *right multiplication* with the matrix

$$R(\mathrm{i}\kappa) = \frac{1}{\sqrt{2\mathrm{i}\kappa}} \begin{bmatrix} 1 & 1 \\ -\kappa & \kappa \end{bmatrix} \tag{16}$$

(see appendix A2). The right multiplication yields a new system of two fundamental solutions with initial data $R(\mathrm{i}\kappa)$. We conjugate *the full transfer matrix* at fixed energy according to

$$M \to \tilde{M} = R^{-1} M R. \tag{17}$$

This new form of the transfer matrix propagates the new system of fundamental solutions. The boundary condition for a bound state requires that an exponentially increasing solution in the left-hand tunnel produces *exclusively an exponentially decaying solution in the right-hand tunnel*. This property must arise already from the transfer matrix of the finite string—we need no asymptotics.

Proposition 5. The finite string has a bound state if and only if at the energy $E(\kappa_0) = -\frac{\hbar^2}{2m}\kappa_0^2$ the lower diagonal element of the new tranfer matrix $\tilde{M}$ vanishes.

Example 1. For the square well equation (2) the new transfer matrix, taken only over the interval $\langle 0, a\rangle$, becomes

$$\tilde{M}(a) = \begin{bmatrix} \cos(ka) + \frac{1}{2}(\frac{k}{\kappa} - \frac{\kappa}{k})\sin(ka), & \frac{1}{2}(\frac{k}{\kappa} + \frac{\kappa}{k})\sin(ka) \\ -\frac{1}{2}(\frac{k}{\kappa} + \frac{\kappa}{k})\sin(ka), & \cos(ka) - \frac{1}{2}(\frac{k}{\kappa} - \frac{\kappa}{k})\sin(ka) \end{bmatrix} \tag{18}$$

and the bound-state condition is

$$\cos(ka) - \frac{1}{2}\left(\frac{k}{\kappa} - \frac{\kappa}{k}\right)\sin(ka) = 0. \tag{19}$$

This equation together with the energy condition always has, as is well known, at least one, in general several, symmetric or antisymmetric solutions.

Now we compare bound states with states in band germs. Consider a fixed bound state with fixed $\kappa = \kappa_0, k = k_0$. Evaluation of the trace of the transfer matrix $M(b + a)$ of the band germ equation (11) at this value yields with the help of equation (19)

$$\tfrac{1}{2}|\operatorname{tr}(M)| = |\cos(k_0 a)| \exp(-\kappa_0 b) < 1. \tag{20}$$

This corresponds to an inner point of a band germ and so we have, first for the square well, a *local implication of K-space for bound states*.

Proposition 6. A bound state whose binding potential is located in a finite string is always embedded into a band germ.

The finite string may also appear as part of a larger string. Because of their specific boundary conditions at the limits of the finite string, we then refer to the former bound states as *decaying states*. Conversely, given a single bound state on a finite string, the band germ energy interval can be reinterpreted as *an energy gauge for the single bound state*. We shall use the term *energy gauge* f for a function of the energy which displays the gaps and band germ intervals of the finite string say with the values 1 or 0 respectively, see figures 1 and 2. The spatial behaviour found in bound and (in two directions exponentially) decaying states will be termed confinement.

The notion of decaying states still refers to a finite string embedded into tunnels of infinite length. Therefore we avoid the term localized state.

At the fixed value $\kappa = \kappa_0$ and corresponding energy $E < 0$ we have now *three types of states*: two Bloch germs with complex conjugate eigenvalues, and the bound state. It follows that *the bound or decaying state must be locally expressible as a superposition of Bloch germs*. Conversely, by adding to the bound-state solution a second non-decaying solution of the same energy, we must be able to construct the two Bloch germs. The contrast between these states appears in the boundary conditions and in the *conserved charge current density*.

For the bound or decaying state we obtain at any point in the tunnel the value $j = 0$, there is no current. In contrast to this, the Bloch germs carry standard charge current according to equation (10) to the right and left respectively.

Example 2. We illustrate the situation by a band germ formed from a δ-potential (3) followed by a tunnel of length b with the transfer matrix (12). We obtain, see appendix A2, a single bound state at $\kappa = \kappa_0 = \frac{u}{2}$. This bound state is symmetric with respect to the position of the δ-potential and in the right-hand tunnel has the exponential form

$$\psi(x) = \cosh(\kappa_0 x) - \sinh(\kappa_0 x) = \exp(-\kappa_0 x). \tag{21}$$

At this energy, we get for M from equation (13) $\frac{1}{2}\operatorname{tr}(M) = \lambda_0 = \exp(-\kappa_0 b)$.

The eigenvalues for the Bloch germs are given by equation (6) with the present value of λ_0. From the explicit form of M at $\kappa = \kappa_0$ we compute, see appendix A1, the two eigenstates for the eigenvalues $\mu, \overline{\mu}$ and obtain in the right-hand tunnel the Bloch germs

$$\begin{aligned}
\phi_1(x) &= \sqrt{\frac{1}{ul}}[\cosh(\kappa_0 x) - \sinh(\kappa_0 x) + \mathrm{i}l\sinh(\kappa_0 x)] \\
\phi_2(x) &= \sqrt{\frac{1}{ul}}[\cosh(\kappa_0 x) - \sinh(\kappa_0 x) - \mathrm{i}l\sinh(\kappa_0 x)] \\
l &:= \frac{\sqrt{1-\exp(-2\kappa_0 b)}}{\sinh(\kappa_0 b)}.
\end{aligned} \tag{22}$$

These states have the standard charge current densities of equation (10). They could be converted to the usual Bloch form by extracting the factors $\exp(\pm \mathrm{i}Kx)$ respectively. Clearly the bound state equation (21) in the tunnel may be expressed as the superposition of Bloch germs,

$$\psi(x) = \tfrac{1}{2}\sqrt{ul}(\phi_1(x) + \phi_2(x)). \tag{23}$$

6. The gauge for crystals: bound states, bands, and Bloch states

We rephrase the well known periodic case [12] in these terms. Consider first the finite string of length $a + b$ with a single atom and with the transfer matrix (11). Repeat this string n times to produce a new transfer matrix M^n. Since the existence of band germs is related to the eigenvalue problem, the range of energies for which $\frac{1}{2}|\operatorname{tr}(M^n)| < 1$ is *independent of* n, *the band germs stay the same on the new string*. The Bloch germs propagate through the string and pick up the same phase factors $\mu, \overline{\mu}$ respectively after each transmission.

Consider next the bound states of the string M^n.

Proposition 7. The bound states of the string M^n may be grouped into sets of n states, where the energies of each such set corresponds to a part $f = 0$ of the energy gauge f of the string M.

Proof. For very tight binding ($ua \gg 1, ub \gg 1$) it suffices to give a proof based on first-order degenerate-perturbation theory, applied to the bound states of the single atoms: to this order, the bound states of the string are the eigenvalues of a matrix whose off-diagonal entries are the weak atom–atom cross terms. By standard matrix theory, the maximum level splitting will increase with n. However, band theory tells us that in the limit $n \to \infty$ all energies stay inside the band, hence inside the initial band germ. Thus the energy of all these bound states for finite n must stay within the energy gauge of the (single) band germ. □

We now have the following situation in the finite string M^n: in a band germ from the string M, there is for each energy value a pair of Bloch germs which can carry charge current. There are now n discrete bound states with the energy gauge as in the initial string.

A schematic view of the periodic scheme is given in figure 1. Now we can extend the analysis to $n \to \infty$.

Proposition 8. For an infinite periodic repetition of a fixed string, the energy gauge stays the same as for the initial string. The band germ generates a band. Within each band there is an *infinite set of (pairs of) Bloch states whose energies* $E_K < 0$ *fill up the original band germ.*

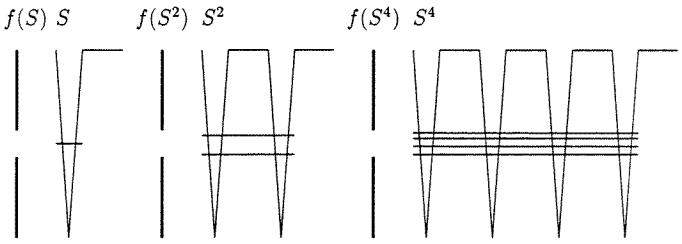

Figure 1. Periodic strings. The string S to the left has one attractive δ-well with a single bound state, followed by a tunnel. The vertical bar to its left shows the energy interval for the band germ. This interval is an energy gauge $f(S)$ comprising the bound state. The string S^2 in the middle has two attractive δ-potentials and two bound states. The energy gauge $f(S^2)$ is unchanged but comprises two bound states. The same energy gauge $f(S^4)$ for the string S^4 to the right comprises four bound states.

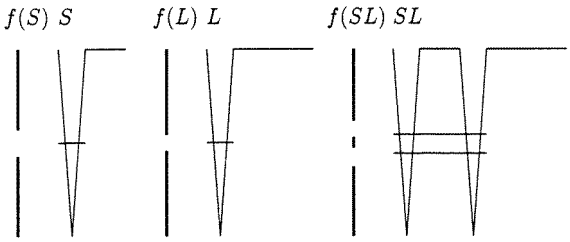

Figure 2. Fibonacci strings. The string S to the left and its energy gauge $f(S)$ are as in figure 1. The string L in the middle has the same bound state within the gauge $f(L)$ of smaller width. The string SL to the right has two δ-wells and hence the same bound states as S^2 in figure 1. In contrast to S^2, the string SL has two separate band germs as in example 3. The corresponding two parts of the energy gauge $f(SL)$ each comprise one bound state but block the energy of the single-atom bound state.

7. Tight binding and energy gauges on Fibonacci strings

We move on to quasiperiodic strings, the basic example being the Fibonacci strings [8, 2]. In contrast to the usual treatment we emphasize the tight-binding scenario. Consider one type of atoms whose potential is an attractive well or a δ-potential equation (3). Assume two spacings and transfer matrices S, L for the potential well followed by tunnels of length $S : b, L : \tau b$ respectively. The Fibonacci string is generated as

$$S \to L \to SL \to LSL \to SLLSL \to LSLSLLSL \ldots . \tag{24}$$

We read these strings as a sequence of intervals on the line running from the left to the right.

Example 3. Consider the Fibonacci string formed by attractive δ-potentials of equal strength at initial points of intervals with length $S \to b, L \to \tau b$ and transfer matrices $M(b+\epsilon), M(\tau b+\epsilon)$ as in equation (12). The third string SL has two δ-potentials at a distance b. By the technique described in section 6 we derive from the transfer matrix the condition for bound states. We are dealing with hybrid states of the double δ-potential. These are symmetric or antisymmetric with respect to the midpoints of the string of length b. The corresponding values $\kappa_{1,2}$ are found as described in section 6. In terms of the parameter

$$\lambda_i := \exp(-\kappa_i b) \tag{25}$$

one finds from appendix A3:

$$\lambda_1 = \frac{2\kappa_1 - u}{u} \qquad \lambda_2 = \frac{-2\kappa_2 + u}{u}. \tag{26}$$

Thus the symmetric bound state is below, the antisymmetric bound state above the single-atom bound state with $\kappa_0 = \frac{u}{2}$.

The trace for the string SL may be written in terms of the parameter $\lambda := \exp(-\kappa b)$ and from appendix A4 becomes

$$\frac{1}{2}\operatorname{tr}(M) = \frac{\kappa+u}{2\kappa}\lambda^{\tau+1} + \frac{\kappa-u}{2\kappa}\lambda^{-\tau-1} + \frac{1}{8}\left(\frac{u}{\kappa}\right)^2(\lambda^{\tau+1} + \lambda^{-\tau-1} - \lambda^{\tau-1} - \lambda^{-\tau+1}). \tag{27}$$

For the bound-state values λ_1, λ_2 one verifies that the absolute value of the half-trace equation (27) is smaller than one so that each one is in a band germ, see figure 3.

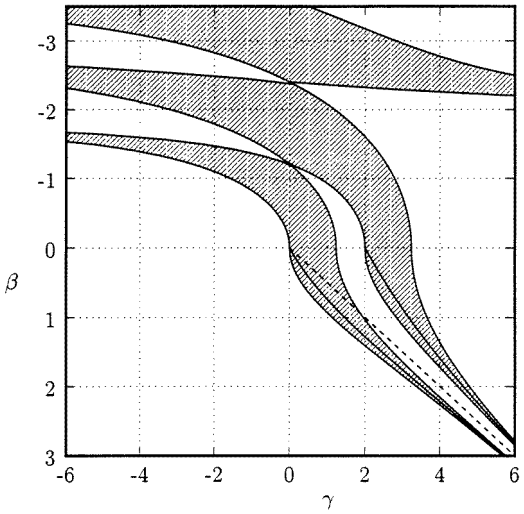

Figure 3. The string SL. Band germs and bound states as functions of the parameters β of the energy and of the parameter γ of the potential strength. The energy is negative in the lower part $\beta > 0$ and positive in the upper part $\beta < 0$. The δ-potentials are attractive for $\gamma > 0$ in the tight-binding scenario, right-hand side, and repulsive for $\gamma < 0$ in the loose binding scenario, left-hand side. Band germs are shaded, bound states of the single and double δ-potential are shown as a dashed line and full curves for $\gamma > 0, \beta > 0$.

We compute the trace equation (27) at the single-atom bound-state value κ_0 and obtain

$$\tfrac{1}{2}\,\mathrm{tr}(M) = 2\lambda_0^{\tau+1} - \tfrac{1}{2}(\lambda_0^{-\tau+1} + \lambda_0^{\tau-1}). \tag{28}$$

For a strength $\gamma := ub = 2\kappa_0 b = 2$ we obtain the value

$$\tfrac{1}{2}\,\mathrm{tr}(M) = -1.18 \tag{29}$$

and so for $\gamma > 2$ the single-atom binding energy is outside the two band germs but in between the two bound states, see figure 3.

From the separation we can estimate the characteristics of energy and distance for this tight-binding scenario: with an assumed distance $b = 1.058 \times 10^{-8}$ cm, the value $\kappa_0 b = 1$ yields a single-atom bound-state energy $E = -3.4$ eV.

In figure 3 we give a complete quantitative description of the string SL as a function of the parameters $\gamma := ub, \beta := \kappa b$. The right-hand part with $\gamma \geqslant 0$ describes the tight-binding scenario. For negative energy $E = -\frac{\hbar^2}{2m}\kappa^2 \leqslant 0, \beta \geqslant 0$ we give the two band germs (shaded). The bound state of the single δ-potential is marked by a broken line. The bound (decaying) states of the attractive double δ-potential are shown as curves running inside the two completely separated band germs which set their energy gauges. For $0 \leqslant \gamma < 2$ there is only one bound state, namely the symmetric hybrid state of the two atoms at distance b. The second antisymmetric hybrid state appears bound only for a strength $\gamma \geqslant 2$. Only for large values of γ do the band germs give good estimates for the two bound (decaying) states.

In the upper part of figure 3 we extend the notion of band germs to positive energy $E = \frac{\hbar^2 k^2}{2m} > 0$ by the analytic continuation $\kappa \to k = -\mathrm{i}\kappa > 0, \beta = -kb < 0$. On the left-hand side of figure 3 with $\gamma < 0$ we include the loose-binding scenario with repulsive δ-potentials of the same spacing. The gaps between the band germs close for vanishing potential $\gamma = 0$ as expected and continue to the positive-energy region studied in this

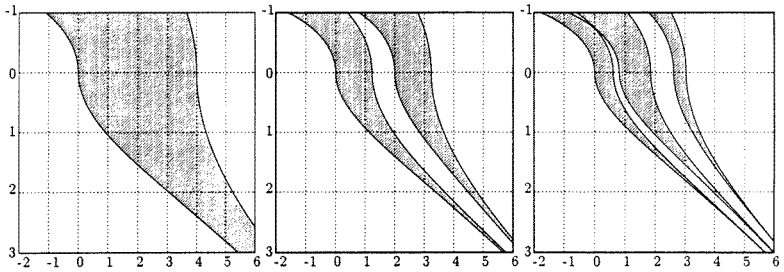

Figure 4. Band germs for the strings S, SL, LSL respectively in a Fibonacci sequence of δ-potentials. The strength and energy parameters are as in figure 3. For negative energy $\beta > 0$ there are one, two and three well-separated band germs respectively. The number of band germs increases with the number of atoms.

scenario. Note, however, that there are no bound or decaying states associated with this type of band germs.

We conclude that the band germs in the Fibonacci string provide the energy gauge for the bound or decaying states of that string but, in marked contrast to the periodic case, have no simple predictive power for the extension of the string. If we considered the string SL as an approximant, we would interprete the band germs as proper bands and derive from them the DOS. This DOS would be a sequence of gaps and in-band density distributions. It would be appropriate for an approximant crystal but yield no helpful information for the quasicrystal.

In figure 4 we display in three parts the changes in the band germs for the first three strings S, SL, LSL of the Fibonacci sequence. The three strings show one, two and three well separated band germs respectively. There is no simple relation between the three band-germ patterns at a fixed strength parameter γ. The number of band germs grows proportionally to the number of atoms. The width of the band germs shrinks with increasing length. In contrast to the periodic case there is no filling of the initial band germs by states under the quasiperiodic extension of the string. For high values of the strength γ the narrow band germs encapsulate the one, two or three bound or decaying states of the strings.

Clearly there is a fundamental difference in the behaviour of gauges for the periodic case discussed in section 6 and for the present quasiperiodic one.

Now we discuss the Fibonacci sequence in terms of the well known trace map [2, 9] which allows to compute the traces of the Fibonacci strings recursively: The set of three successive half-traces forms a discrete dynamical system which has an invariant I related to the commutator

$$K(M(\tau b+\epsilon), M(b+\epsilon)) := M(\tau b+\epsilon)M(b+\epsilon)M^{-1}(\tau b+\epsilon)M^{-1}(b+\epsilon) \tag{30}$$

by

$$\tfrac{1}{2}\,\mathrm{tr}(K) = 2I + 1. \tag{31}$$

The geometry and meaning of this invariant is discussed for example in [8, 2, 9, 10]. It determines a cubic surface in the space of the three half-traces, whose shape depends on the value of the half-trace of the commutator. In [2] it was shown that this invariant as a function of k has quadratic zeros with period $k = \frac{\pi}{(\tau-1)b}$. This value of I implies for the trace map that the cubic surface develops a part bounded by the unit cube and for the two transfer matrices that they commute. It was shown in [2] numerically that at the corresponding energies one should expect extended states.

The analysis of [2] was carried out exclusively in the *loose-binding scenario*. In the present *tight-binding scenario there are important changes*: the trace of the commutator can be obtained by analytic continuation from the value given in [2] and now yields, (see appendix A3),

$$\frac{1}{2}\,\mathrm{tr}(K) = 1 + \frac{1}{2}\left(\frac{u}{\kappa}\right)^2 (\sinh(\kappa(\tau-1)b))^2. \tag{32}$$

Proposition 9. In the tight-binding scenario on Fibonacci strings with a single type of δ-well on each vertex, the invariant I is always larger than zero. The cubic surface for the trace map has no bounded part, it corresponds to figure 1 of [8]. No pair of transfer matrices can commute.

From this analysis we see that, when we start in the band germ of the string S, L and hence have half-traces of absolute value smaller than one to begin with, we can already get in the next string SL, a half-trace of absolute value larger than one. This happens in example 3 at the single-atom binding energy. It essentially implies that the dynamical system of half-traces at this fixed initial energy can, and in general will, leave the region of the invariant surface I bounded by the unit cube. There are no regions of fixed energy where we can expect extended states. The only energetic positions where half-traces of absolute value smaller than one can occur are the band germs associated with the bound or decaying states. These band germs under extension of the quasiperiodic string and as functions of the energy develop in a non-trivial fashion. The quasiperiodic DOS is governed by this development.

We summarize the results obtained from the Fibonacci tight-binding scenario.

Proposition 10. The transfer matrix for any string in the tight-binding scenario after n steps may have up to n separate band germs. These band germs gauge up to n bound or decaying states. Under the quasiperiodic extension of the string, the system of band germs keeps changing. In this extension, the change of the one-electron DOS cannot be described and labelled by the filling of the system of band germs obtained in step n. The development of the system of band germs follows the pattern of decaying states for the finite strings. The distribution of these decaying states under the quasiperiodic extension should play a crucial role for the shape and interpretation of the DOS in quasicrystals.

A single electron assigned to a band germ could occupy the decaying state, would be confined to the quasicrystal and carry vanishing charge current density.

8. Electron confinement

The present analysis provides some new concepts for electron states in quasicrystals and in particular a new interpretation for the tight-binding approximant scheme. The concepts and the interpretation of course still have to be tested and established by model computations in systems of 3D. In 3D we consider a quasicrystal made up by the quasiperiodic packing of elementary patches into larger patches.

(i) The bands computed from an approximant can be reinterpreted as *band germs of finite patches*. Each band germ of the patch *opens up an interval on the energy gauge for a single bound state*. It would provide a set of one-electron band energies and a corresponding DOS with gaps and in-band parts only if the patch were repeated periodically so that the Bloch germs could match. This only happens in an approximant crystal. For a quasicrystal the DOS cannot be obtained by interpreting the band germs as proper bands.

(ii) It makes sense to consider the bound states of free clusters taken from a quasicrystal, [11] since these bound states can yield information on relevant decaying states.

(iii) In building a quasiperiodic structure, the Bloch germs from the patches in general do not match one another. Each bound state of an isolated patch when built into a larger patch could become a decaying and hence a confined state. In a tight binding scenario, the number of band germs and hence of these decaying states can increase proportionally to the number of atoms. The DOS of the quasicrystal must be found from the development of the band germs under quasiperiodic extension. This development is closely linked to the distribution of decaying states.

Electrons in band germs could occupy these decaying or confined states of vanishing charge current density, part of which could be assigned to hybrid states in local clusters.

Appendix A

A.1. Charge current density

We first derive equation (10) for the charge current. Normalization of the current density replaces the norm for these solutions which are not square integrable. A matrix $g_c \in SU(1,1)$ with $\frac{1}{2}|\operatorname{tr}(g_c)| < 1$ has two complex conjugate eigenvalues $\mu, \overline{\mu}$ and eigenvectors as given in the columns of the matrix V_c equation (7). We identify the real form $g = qg_cq^\dagger$ with a transfer matrix

$$MqV_c = qV_c\Delta = \sqrt{\frac{1}{2}}\begin{bmatrix} v+w & \overline{w}+\overline{v} \\ \mathrm{i}(v-w) & \mathrm{i}(\overline{w}-\overline{v}) \end{bmatrix}\begin{bmatrix} \mu & 0 \\ 0 & \overline{\mu} \end{bmatrix}. \tag{33}$$

Computation of the charge current density yields from the first column of this matrix

$$j_1 = \frac{e\bar{h}}{2\mathrm{i}m}(\overline{\phi}_1\phi_1' - \overline{\phi}_1'\phi_1) = \frac{e\bar{h}}{2m}(v\overline{v} - w\overline{w}) = \frac{e\bar{h}}{2m}. \tag{34}$$

A.2. Bound states and Bloch germs

The matrix equation (4) yields upon right multiplication with R from equation (16) the new fundamental system

$$MR = \frac{1}{\sqrt{2\mathrm{i}\kappa}}\begin{bmatrix} \exp(-\kappa x) & \exp(\kappa x) \\ -\kappa\exp(-\kappa x) & \kappa\exp(\kappa x) \end{bmatrix} \tag{35}$$

of exponentially de- and increasing functions. The new transfer matrix of this fundamental system for the transfer matrix equation (3) of the δ-well is

$$\tilde{M}(\epsilon) = R^{-1}M(\epsilon)R = \frac{1}{2\kappa}\begin{bmatrix} 2\kappa+u & u \\ -u & 2\kappa-u \end{bmatrix}. \tag{36}$$

For a bound state the lower diagonal part of this matrix must vanish and so $2\kappa_0 - u = 0$. Consider now the band germ $M(b+\epsilon)$ equation (12) at this energy. Its half-trace at $\kappa = \kappa_0$ becomes $\lambda_0 = \exp(-\kappa_0 b)$ and the eigenvalues are given by equation (6). A similar computation for the transfer matrix equation (2) yields equations (18) and (19).

To compute a Bloch germ of $M(b+\epsilon)$ from equation (12) we determine it as the eigenvector (c_1, c_2) for the eigenvalue μ at the single-atom bound-state energy with $\kappa_0 = \frac{u}{2}$ from

$$\begin{aligned} &(\cosh(\kappa_0 b) - 2\sinh(\kappa_0 b) - \mu)c_1 + \frac{2}{u}\sinh(\kappa_0 b)c_2 = 0 \\ &\frac{c_2}{c_1} = \frac{u}{2}(1+\mathrm{i}l) \\ &l := \frac{\sqrt{1-\exp(-2\kappa_0 b)}}{\sinh(\kappa_0 b)}. \end{aligned} \tag{37}$$

The first Bloch germ in the right-hand tunnel with this ratio of coefficients becomes

$$\phi_1 \sim \cosh(\kappa_0 x) - \sinh(\kappa_0 x) + \mathrm{i}l \sinh(\kappa_0 x)). \tag{38}$$

Upon normalizing the charge current according to equation (10) one finds the upper part of equation (22).

A.3. Fibonacci strings

The string with transfer matrix $M(\tau b + \epsilon)M(b + \epsilon)$ has the bound states of two δ-wells at a distance b. Transforming the product $M(\epsilon)M(b)M(\epsilon)$ from equations (3) and (4) with the matrix R and putting the lower diagonal element equal to zero yields

$$2(\kappa - u)\cosh(\kappa b) + \left(2(\kappa - u) + \frac{u^2}{\kappa}\right)\sinh(\kappa b) = 0. \tag{39}$$

With $\lambda_i := \exp(-\kappa_i b)$ one finds for the symmetric solutions

$$\lambda_1 = \frac{2\kappa_1 - u}{u} \tag{40}$$

and for the antisymmetric solutions

$$\lambda_2 = \frac{-2\kappa_2 + u}{u}. \tag{41}$$

For the string SL the transfer matrix is a product

$$M = M(b_2 + \epsilon)M(b_1 + \epsilon) \tag{42}$$

of two transfer matrices of the type equation (12). We give the general matrix elements of this product:

$$\begin{aligned}
M_{11} &= \cosh(\kappa b_2)\cosh(\kappa b_1) + \left(1 + \left(\frac{u}{\kappa}\right)^2\right)\sinh(\kappa b_2)\sinh(\kappa b_1) \\
&\quad -\frac{u}{\kappa}\cosh(\kappa b_2)\sinh(\kappa b_1) - \frac{2u}{\kappa}\sinh(\kappa b_2)\cosh(\kappa b_1) \\
M_{12} &= -\frac{u}{\kappa^2}\sinh(\kappa b_2)\sinh(\kappa b_1) \\
&\quad +\frac{1}{\kappa}\cosh(\kappa b_2)\sinh(\kappa b_1) + \frac{1}{\kappa}\sinh(\kappa b_2)\cosh(\kappa b_1) \\
M_{21} &= -2u\cosh(\kappa b_2)\cosh(\kappa b_1) - u\sinh(\kappa b_2)\sinh(\kappa b_1) \\
&\quad +\left(\kappa + \frac{u^2}{\kappa}\right)\cosh(\kappa b_2)\sinh(\kappa b_1) + \kappa\sinh(\kappa b_2)\cosh(\kappa b_1) \\
M_{22} &= \cosh(\kappa b_2)\cosh(\kappa b_1) + \sinh(\kappa b_2)\sinh(\kappa b_1) - \frac{u}{\kappa}\cosh(\kappa b_2)\sinh(\kappa b_1).
\end{aligned} \tag{43}$$

For the string SL we have $b_1 = \tau b, b_2 = b$. The half-trace in terms of $\lambda := \exp(-\kappa b)$ becomes

$$\begin{aligned}
\frac{1}{2}\mathrm{tr}(M) &= \cosh((\tau+1)\kappa b) - \frac{u}{\kappa}\sinh((\tau+1)\kappa b) + \frac{1}{2}\left(\frac{u}{\kappa}\right)^2\sinh(\tau\kappa b)\sinh(\kappa b) \\
&= \frac{\kappa + u}{2\kappa}\lambda^{\tau+1} + \frac{\kappa - u}{2\kappa}\lambda^{-\tau-1} + \frac{1}{8}\left(\frac{u}{\kappa}\right)^2(\lambda^{\tau+1} + \lambda^{-\tau-1} - \lambda^{\tau-1} - \lambda^{-\tau+1})
\end{aligned} \tag{44}$$

which is equation (27). By the use of two general products as in equation (43) one can compute the commutator equation (30) and obtain its half-trace equation (32).

Acknowledgments

The author wishes to thank the referees of the first version of this manuscript for their critical comments. He would also like to thank Tobias Kramer for assistance in the computational and graphical part.

References

[1] Ashcroft N W and Mermin N D 1976 *Solid State Physics* (Philadelphia, PA: Saunders)
[2] Baake M, Joseph D and Kramer P 1992 *Phys. Lett.* A **168** 199–208
[3] Fujiwara T and Yokokawa T 1991 *Phys. Rev. Lett.* **66** 333–6
[4] Fujiwara T, Mitsui T, Yamamoto S and Trambly de Laissardiere G 1995 *Proc. 5th Int. Conf. Quasicrystals* ed Ch Janot and R Mosseri (Singapore: World Scientific) pp 393–400
[5] Heine V 1980 Electronic structure from the point of view of the local environment *Solid State Physics* vol 35, ed F Seitz and D Turnbull (New York: Academic) pp 1–127
[6] Haydock R 1980 The recursive solution of the Schrödinger equation *Solid State Physics* vol 35, ed F Seitz and D Turnbull (New York: Academic) pp 215–94
[7] Janot Ch and Mosseri R 1995 *Proc. 5th Int. Conf. Quasicrystals* (Singapore: World Scientific) pp 389–624
[8] Kohmoto M 1987 *Int. J. Mod. Phys.* B 31–49
[9] Kramer P 1993 *J. Phys. A: Math. Gen.* **26** 213–28
[10] Kramer P 1993 *J. Phys. A: Math. Gen.* **26** L245–50
[11] Kramer P, Quandt A, Schlottmann M and Schneider T 1995 *Phys. Rev.* B **51** 8815–29
[12] Lieb E H and Mattis D C 1966 *Mathematical Physics in One Dimension* (New York: Academic)
[13] Skriver H L 1984 The LMTO method: muffin-tin orbitals and electronic structure *Springer Series in Solid State Sciences* (Berlin: Springer)
[14] Stadnik Z, Purdie D, Garnier M, Baer Y, Tsai A-P, Inoue A, Edagawa K and Takeushi S 1996 *Phys. Rev. Lett.* **77** 1777
[15] Wigner E P and Seitz F 1933 *Phys. Rev.* **43** 804–10
Wigner E P and Seitz F 1934 *Phys. Rev.* **46** 509–24